Electronic supplementary materials *Mendeleev Commun.*, 2026, **36**, 138–141

New abiraterone analogue with atypical position of N-heterocyclic substituent: synthesis, crystal structure and CYP17A1/CYP3A4 binding affinity

Evgeniya V. Nurieva, Elena V. Britikova, Anna V. Sydoriuk, Taisiya A. Antonenko, Alexandra V. Mamaeva, Nikolay A. Zefirov, Anastasiya V. Zazdravnykh, Victor A. Tafeenko, Eduard V. Bocharov, Vladimir V. Britikov, Elena R. Milaeva and Olga N. Zefirova

1. Molecular modeling

Molecular docking of compound **8** was performed using a 3D model of the abiraterone binding site in CYP17A1 (PDB ID: 3RUK). All water molecules and abiraterone were removed from the model before docking procedure. The protein atoms were charged according to the standard Kollman method using the AutoDock Tools 1.5.6 program.[S1] The 2D structures of the ligands were transformed into 3D ones, and the geometry was optimized by molecular mechanics in the Amber ff14SB force field using the Gasteiger charge model in the USCF Chimera 1.15 software.[S2] The docking procedure was carried out using the AutoDock Vina 1.1.2 software[S1] (grid box size: 15.0 Å×28.5 Å×18.0 Å with grid center size x = 26.358 Å, y = –0.048 Å, z = 33.783 Å, energy range = 4, exhaustiveness = 30). The resulting complexes corresponding to two clusters of solutions (with the best values of scoring functions) were visualized using UCSF Chimera 1.15 software[S2] (Figure S1).

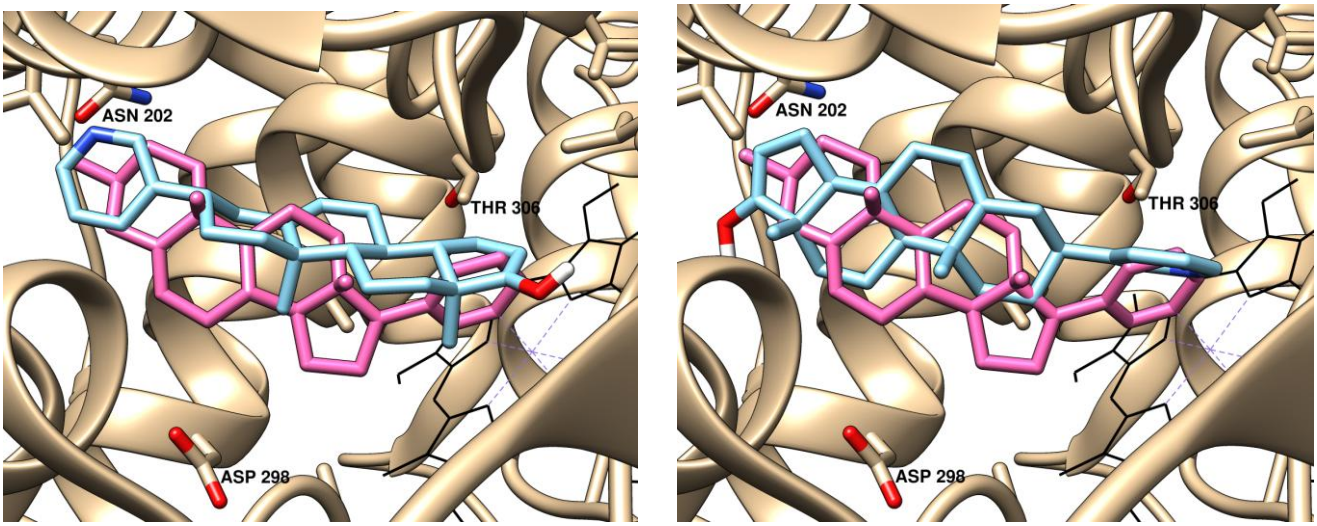

Docking pose 1 Docking pose 2

Figure S1 Complexes of CYP17A1 (PDB ID: 3RUK) with abiraterone (shown in pink) and compound **8** (shown in blue). Heme is displayed by thin black lines. In the docking pose 1, the molecule **8** is inverted relative to the parent compound, while in docking pose 2, the arrangement of both molecules is close and their pyridine rings are located in the protein near the heme iron atom.

2. Chemistry

All solvents were technical grade and distilled from standard drying agents. The starting materials and reagents – 5-androsten-3β-ol-17-one (androstenolone, **5**), 2-bromopyridine, 1,1'-carbonyldiimidazole (CDI), (3β)-17-iodoandrosta-5,16-dien-3-ol (**9**), N,N-diisopropylethylamine (DIPEA), imidazole, *etc.* were purchased as high-grade commercial products (Cayman Chemical, Sigma-Aldrich, Chemieliva Pharmaceutical) and used without further purification. Liquid column flash- or conventional chromatography was performed using silica gel "Macherey–Nagel" (0.063–0.2 мм). Thin-layer chromatography (TLC) was performed on ALUGRAM Xtra G/UV254 silica gel sheets. ^{1}H and ^{13}C NMR spectra were recorded on Agilent 400-MR spectrometer (400.0 MHz for ^{1}H; 100.6 MHz for ^{13}C) at 28 °C. Chemical shifts (δ) are reported in ppm referenced to residual solvent peak ($CDCl_3$, δ_H=7.24 ppm, δ_C=77.0 ppm; methanol-d_4, δ_H = 4.87 ppm, δ_C = 49.15 ppm); spin-spin coupling constants (*J*) are reported in Hz. Liquid chromatography (LC) and ElectroSpray ionization mass spectrometry (ESI-MS) data were obtained on an Agilent 1100 LC/MSD with an Agilent 1100 SL quadrupole mass spectrometer, eluting with 0.05 % TFA in H_2O and 0.05 % TFA in MeCN (positive-ion monitoring mode). CHN elemental analysis was performed using a Carlo-Erba ER-20 analyzer. IR-spectra were registered on FT-IR Termo Nicolet IR200 Spectrometer with 4 cm^{-1} resolution, absorption bands are given in cm^{-1}. Melting points were determined using a capillary melting point apparatus and were uncorrected.

An attempt to synthesize **(3β)-17-hydroxy-3-(pyridin-3-yl)androsta-5,16-diene**.

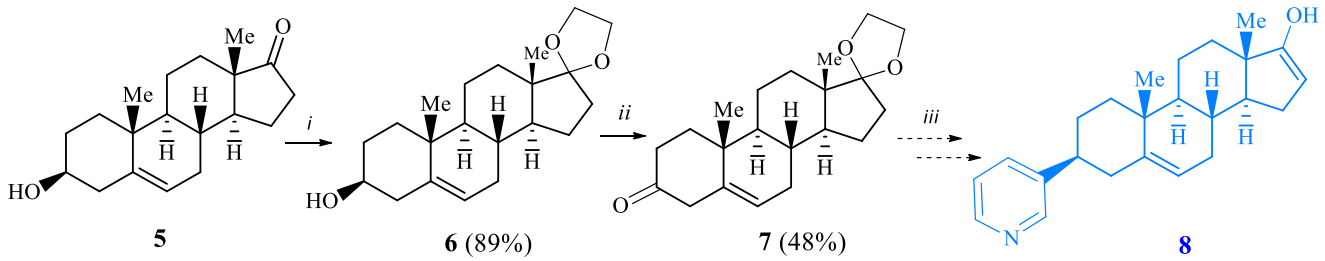

5 **6** (89%) **7** (48%) **8**

5-Androsten-3β-ol-17-one 17-ethylene ketal (**6**) and 5-androsten-3,17-dione 17-ethylene ketal (**7**) were synthesized similar to standard literature procedures, spectral data coincided with the data reported.[S3] A solution of compound **7** (0.078 g, 0.24 mmol) and 2,6-lutidine (30 μL, 0.26 mmol, 1.1 eq) in dichloromethane (5 mL) was cooled to 0 °C under atmosphere of argon and treated with triflic anhydride (44 μL, 0.26 mmol, 1.1 eq) dropwise during 10 min. The mixture was stirred at 0°C during 1 h, then warmed to room temperature within 2 h. The solvent was evaporated under reduced pressure

and the residue redissolved in 1,4-dioxane (10 ml). The solution obtained was degassed with argon, mixed with 3-pyridylboronic acid (0.044 g, 0.36 mmol, 1.5 eq), Na_2CO_3 (0.076 g, 0.72 mmol, 3 eq), LiCl (0,002 g, 0,04 mmol, 0.2 eq) and additionally degassed with argon. Then $(PPh_3)_4Pd$ (0.028 g, 0.024 mmol, 0.1 eq) was added, and the reaction mixture was heated at 90 °C during 12 h. The mixture was diluted with water (50 mL) and extracted with ethyl acetate (2×20 ml). The combined organic layers were dried over Na_2SO_4, concentrated under reduced pressure to give the complex mixture of products, which was chromatographed on silica gel (eluent: ethyl acetate – petroleum ether 40–70 °C, 1:3), the fractions were controlled by ^{1}H NMR and LC-MS analysis, but no C^3-Py comprising precursor of the target product was detected.

(3β)-Androst-5-en-3-ol (10) was obtained by H_2/Ranay nickel reduction of (3β)-17-iodoandrosta-5,16-dien-3-ol (**9**) as described[S4] to give **10** as beige crystals with T.пл. = 130 – 133 °C (Lit. data m.p. 142 – 143 °C[S5]). In ref.[S4] no spectral data were presented.

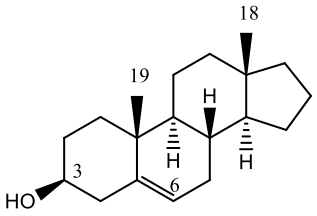

<u>^{1}H NMR (δ, $CDCl_3$)</u>: 0.72 (с, 3 H, H18); 0.87 – 1.00 (м, 2 H); 1.02 (с, 3 H, H19); 1.05 – 1.21 (м, 4 H); 1.39 –1.69 (м, 9 H); 1.73 – 1.77 (м, 1 H); 1.82 – 1.89 (м, 2 H); 1.98 – 2.05 (м, 1 H); 2.21 – 2.33 (м, 2 H); 3.49 – 3.57 (м, 1 H, H3); 5.36 (дд, 1 H, H6, *J* = 4.0, 1.5).

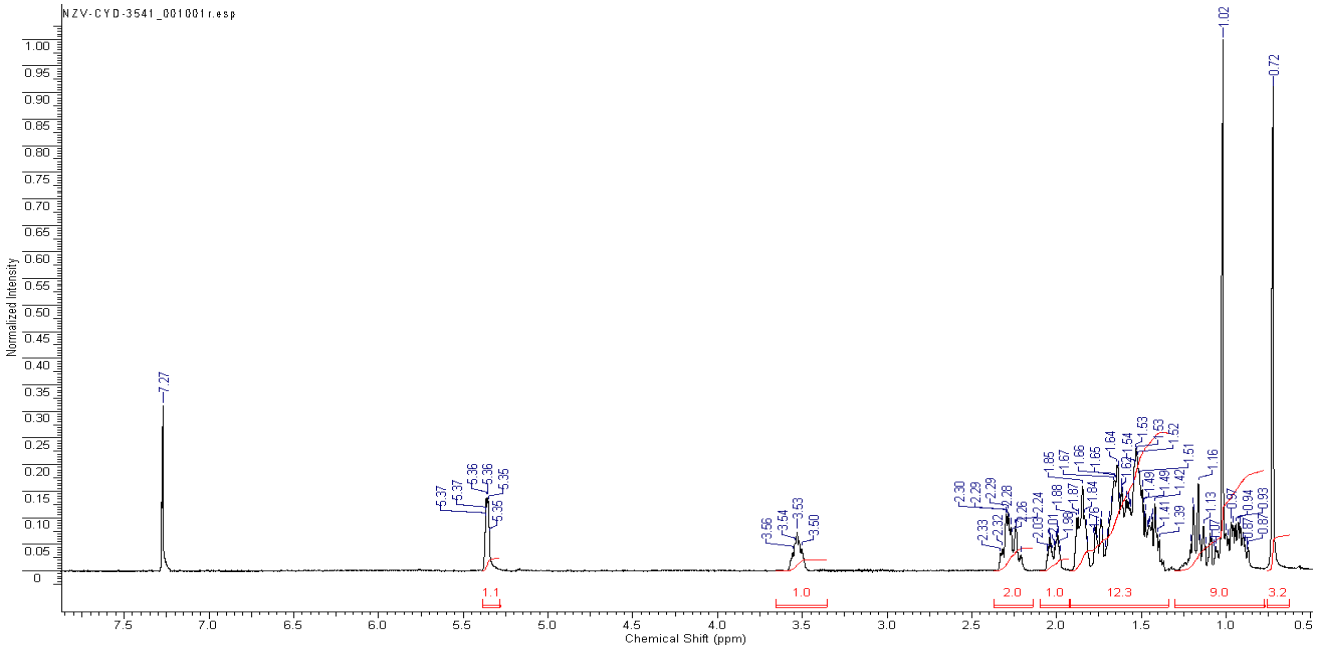

Figure S2 ^{1}H NMR spectrum of compound **10**.

<u>IR spectrum (KBr, cm^{-1})</u>: 801, 844, 954, 1034, 1052, 1166, 1353, 1363, 1375, 1398, 1420, 1463, 2679, 2760, 2844, 2867, 2931, 3222 (O-H broad).

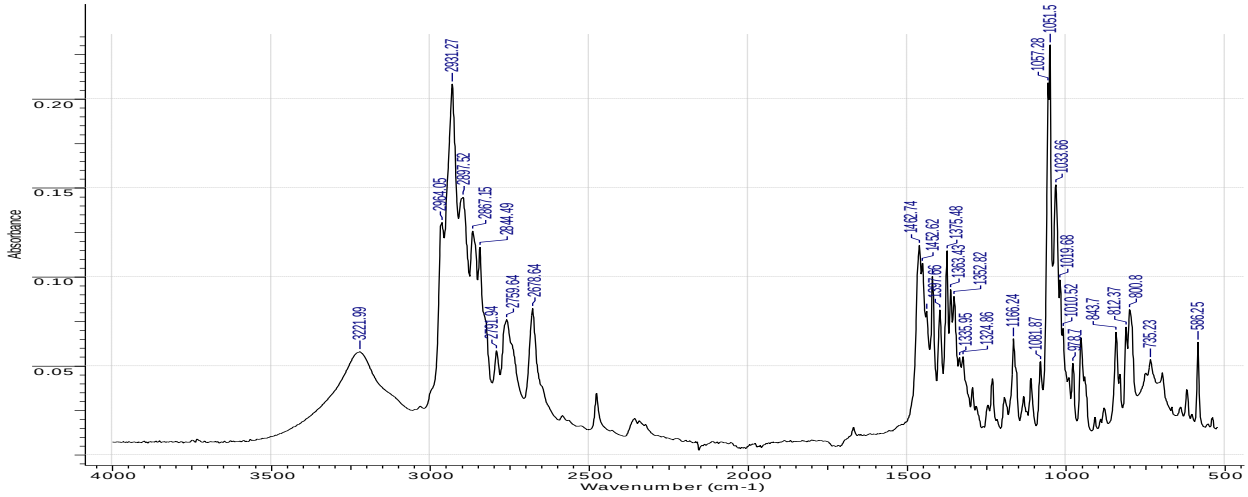

Figure S3 IR spectrum of compound **10**.

(3β)-Androst-5-en-3-yl methanesulfonate (11). A solution of (3β)-androst-5-en-3-ol **10** (0.500 g, 1.82 mmol) and DIPEA (0.352 g 2.73 mmol) in dichloromethane (20 ml) was filled with argon, placed in an ice-cooling bath and mesyl chloride was added dropwise (0.311 g, 2.73 mmol) at a temperature not exceeding 15 °C. The mixture was warmed to room temperature, stirred for 24 h and then washed with brine (3×20 ml). The organic layer was dried over Na_2SO_4, the solvent was evaporated under reduced pressure to give **11** as beige crystals (0.594 g, yield 93%). M.p. 91 – 94 °C.

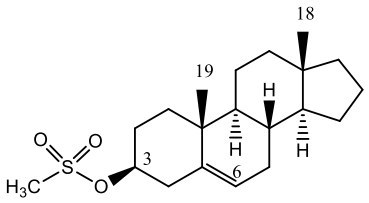

^{1}H NMR (δ, $CDCl_3$): 0.73 (s, 3 H, H18); 0.88 – 1.01 (m, 2 H); 1.04 (s, 3 H, H19); 1.11 – 1.86 (m, 14 H); 1.93 (dt, 1 H, *J* = 13.6, 3.5); 2.01 – 2.07 (m, 2 H); 2.50 – 2.54 (m, 2 H); 3.02 (s, 3 H, CH_3SO_2); 5.44 (dd, 1 H, H6, *J* = 2.3, 1.7).

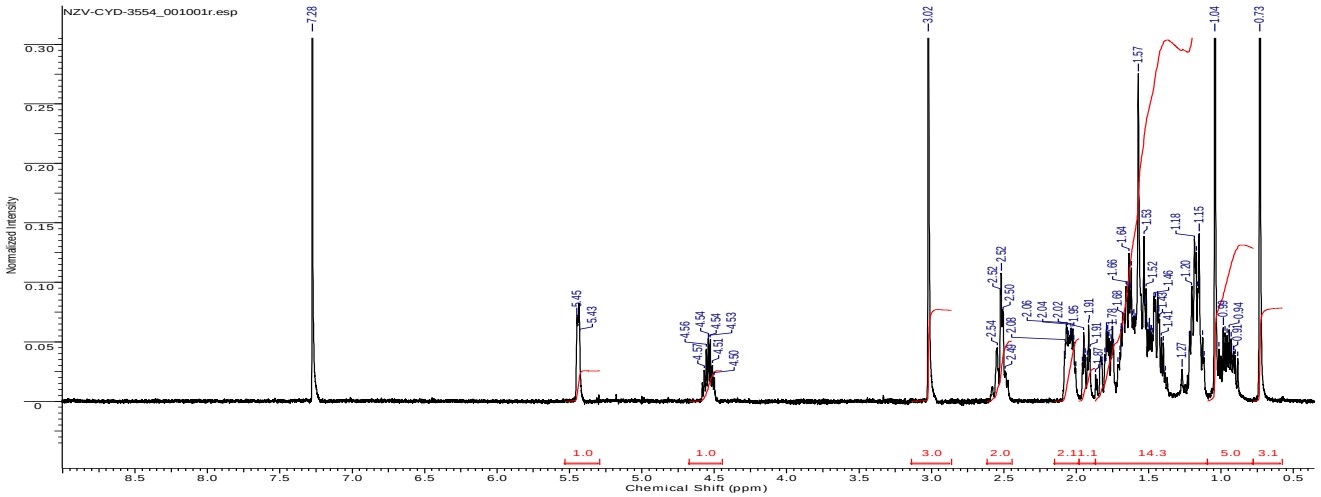

Figure S4 ^{1}H NMR spectrum of compound **11**.

^{13}C NMR (δ, $CDCl_3$): 17.2 (C18), 19.2 (C19), 20.4, 21.0, 25.5, 28.9, 32.0, 32.1, 36.5, 36.9, 38.5 (CH_3SO_2), 38.7, 39.1, 40.2, 40.5, 50.2, 54.7, 82.0 (C3), 123.8 (C6), 138.6 (C5).

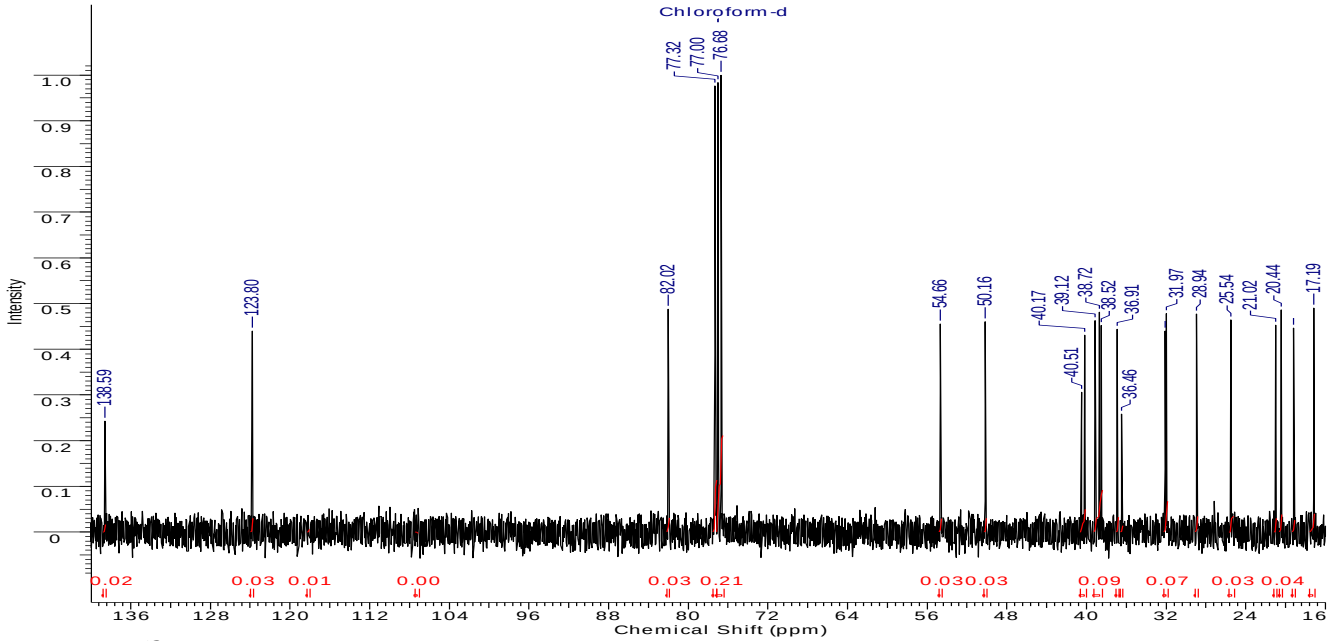

Figure S5 ^{13}C NMR spectrum of compound **11**.

IR spectrum (KBr, cm^{-1}): 813, 835, 864, 926, 945, 1163 (SO_2), 1321, 1349, 1451, 2868, 2908, 2942.

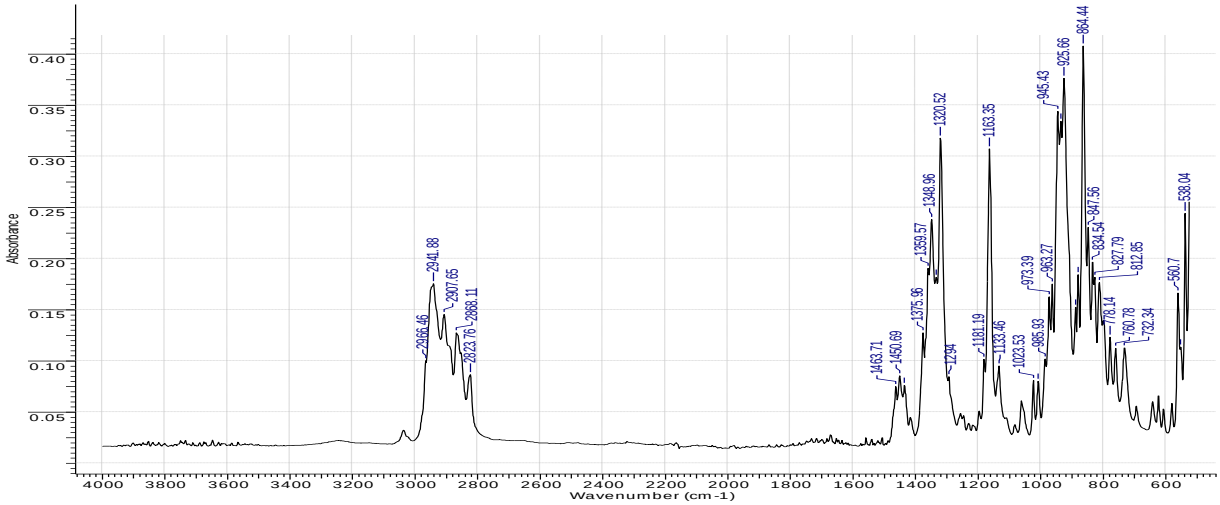

Figure S6 IR spectrum of compound **11**.

MS (ESI), m/z: 353.5 [M+H]. Calculated for $C_{20}H_{33}O_3S$: 353.2.

1-[(1a*R*,3a*R*,3b*S*,5a*S*,8a*S*,8b*S*,10*R*,10a*R*)-3a,5a-Dimethylhexadecahydrocyclopenta[*a*]cyclopropa[2,3]cyclopenta[1,2-*f*]naphthalen-10-yl]-1*H*-imidazole (12). A solution of (3β)-androst-5-en-3-yl methanesulfonate (**11**) (0.270 g, 0.77 mmol) and imidazole (0.156 g, 2.3 mmol) in toluene (50 ml) was refluxed at 110°C 24 h and then cooled to room temperature. LCMS chromatogram (monitored at 254 nm) of crude product mixture revealed the presence of three products with similar molecular ions [M+H] = 325.9 in the ratio ~3:1:6.

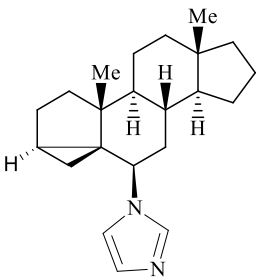

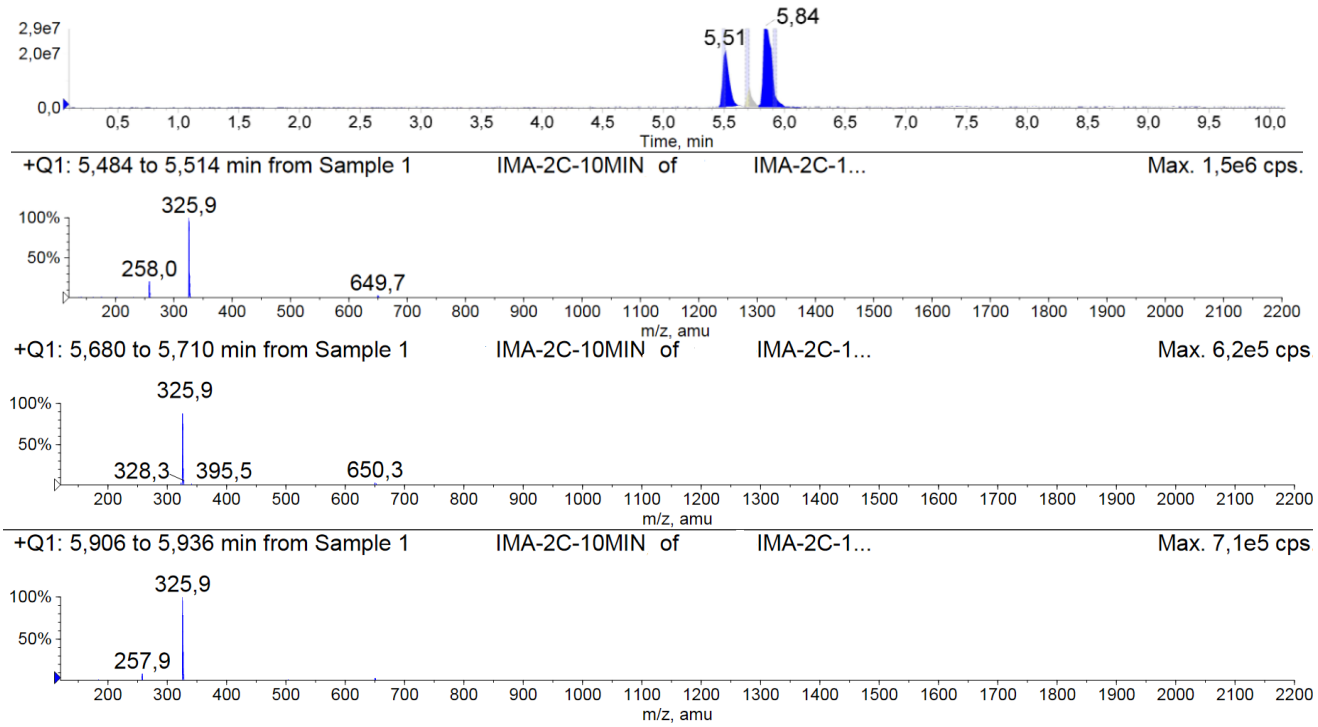

Figure S7 LCMS chromatogram (monitored at 254 nm) of crude product mixture in the reaction of (3β)-androst-5-en-3-yl methanesulfonate **11** with imidazole. Three products with similar molecular ions [M+H] = 325.9 in the ratio ~3:1:6 are observed.

The reaction mixture was washed with brine (3×20 ml), and the organic layers were combined, dried over Na_2SO_4 and concentrated under reduced pressure. The residue was chromatographed (eluent: ethyl acetate – petroleum ether 40–70 °C, 1:5 – 1:2) to give only one analytically pure product **12** as white crystals (0.040 g, yield 16%). M.p. 152 – 154 °C.

Possible mechanism of compound **12** formation (according to data[S6] for structurally similar compounds) is presented at Figure S8.

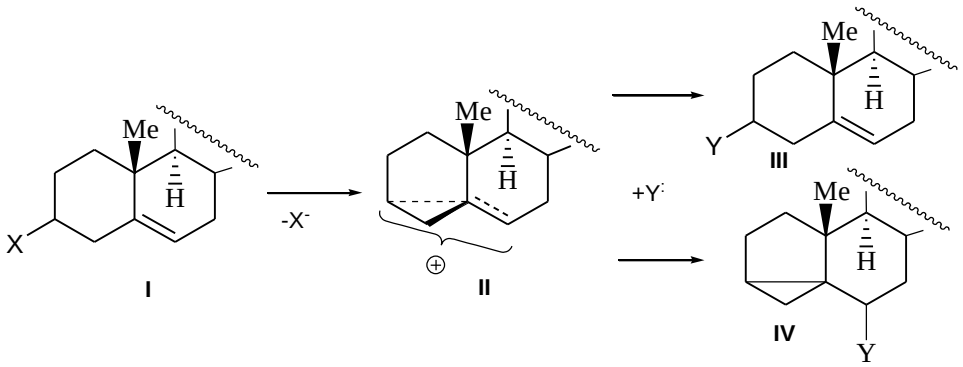

Figure S8 Schematic representation of reaction mechanism of 3-substituted steroid-like compounds comprising 5,6-double bond (**I**) with nucleophiles. Reaction passes *via* formation of homoallylic resonance carbocation (**II**) yielding C^3-substituted derivatives (**III**) or 3,5-cyclosteroids (**IV**).

^{1}H NMR (δ, $CDCl_3$): 0.66 – 0.73 (m, 1 H); 0.68 (s, 3 H, H18); 0.72 (s, 3 H, H19); 0.94 – 1.07 (m, 4 H); 1.11 – 1.36 (m, 5 H); 1.45 – 1.90 (m, 11 H); 2.39 (d, 1 H, *J* = 13.45); 3.56 (s, 1 H, H6); 7.04 (s, 1 H, H4Im); 7.17 (s, 1 H, H5Im); 7.79 (s, 1 H, H2Im).

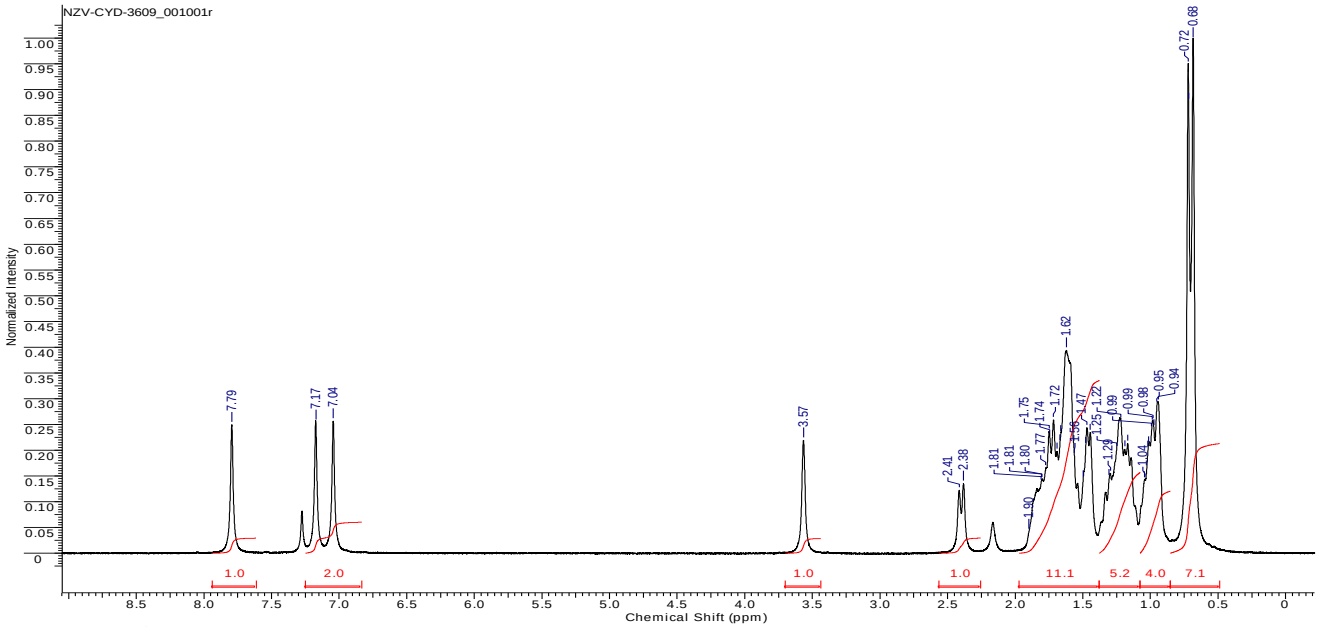

Figure S9 ^{1}H NMR spectrum of compound **12**.

^{13}C NMR (δ, $CDCl_3$): 13.9 (C19), 17.2 (C18), 19.3, 20.2, 22.2, 23.9, 24.2, 25.0, 30.6, 33.1, 34.6, 34.9, 38.4, 39.9, 40.5, 42.8, 47.9, 53.8, 58.5 (C6), 117.8 (C5Im), 128.0 (C4Im), 136.1 (C2Im).

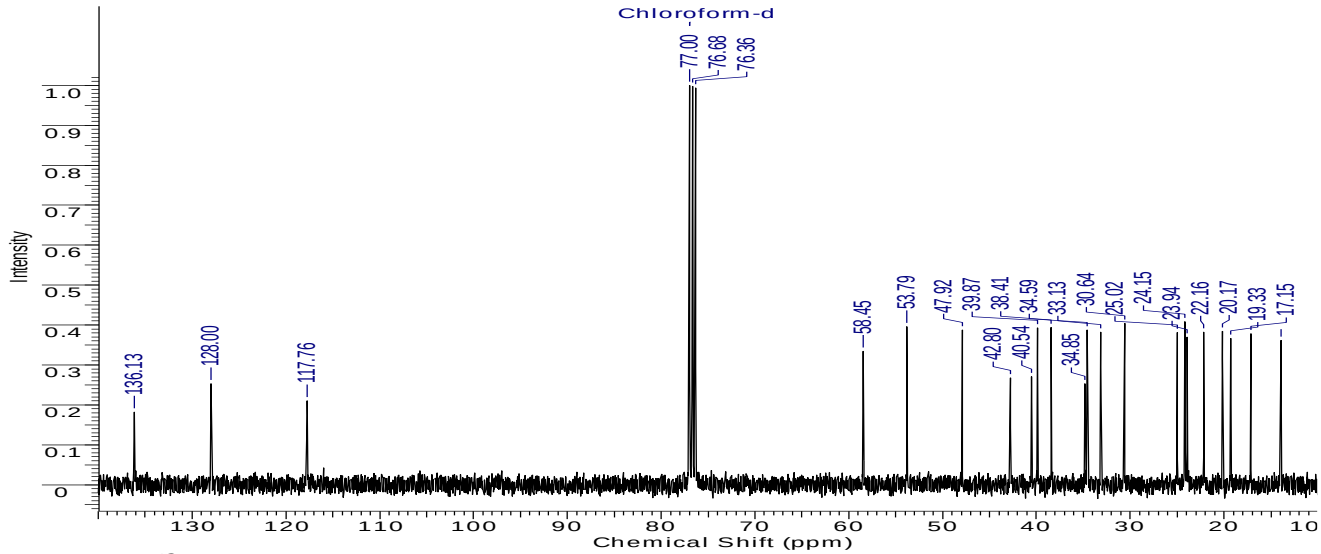

Figure S10 ^{13}C NMR spectrum of compound **12**.

MS (ESI), m/z: 325.9 [M+H], 257.8. Calculated for $C_{22}H_{33}N_2$: 325.5.

Anal. Calcd for $C_{22}H_{32}N_2$: C, 81.43; H, 9.94; N, 8.63. Found: C, 81.49, H, 9.89.

3. Data of X-ray analysis of 1-((1a*R*,3a*R*,3b*S*,5a*S*,8a*S*,8b*S*,10*R*,10a*R*)-3a,5a-dimethylhexadecahydrocyclopenta[*a*]cyclopropa[2,3]cyclopenta[1,2-*f*]naphthalen-10-yl)-1*H*-imidazole (**12**).

Table S1. Crystallographic characteristics, experimental details for compound **12.**

Compound number	**12**
Formula	$C_{44}H_{64}N_4$
Mol. mass	648.99
Space group	$P2_12_12_1$
Crystal system	Orthorhombic
T, K	295(2)
a (Å)	11.1602(4)
b (Å)	12.1569(4)
c (Å)	27.69000(10)
V (Å^3)	3756.80(18)
Z	4
$\Delta\rho_{max}/\Delta\rho_{min}$ (*e*/Å^3)	0.155/-0.131
λ	CuKα
μ (mm^{-1})	0.499
R_1/wR_2 ($I \geq 2\sigma(I)$)	0.0372/0.0696
GOOF	0.783
θ range (°)	4.841 – 65.940
Crystal size (mm)	0.2 × 0.1 × 0.2

4. Biochemical Assay

Recombinant protein expression and purification. Human CYP17A1 Δ2-19 variant[S7] with C-terminal four-residue histidine tag was obtained as described.[S8] In brief, CYP17A1 was expressed in *E. coli* JM109 cells using pCWori based plasmid vector. The target protein was purified from cell lysate using immobilized metal affinity chromatography (IMAC) followed by size-exclusion chromatography. The final protein concentration was determined by measuring change in absorbance after carbonyl complex formation in reduced state (ε_{450} 91000 $M^{-1}\cdot cm^{-1}$).

Human CYP3A4 Δ3−12 S18F variant (NF14)[S3] with with C-terminal six-histidine tag was also expressed in JM109 cells using pCW-LIC plasmid expression vector. Expression, isolation and purification procedure for CYP3A4 were the same as for CYP17A1, but the final purified CYP3A4 preparation contained 0.1 M potassium phosphate buffer (pH 7.4), 20% glycerol, 0.2% CHAPS and 0.3 M NaCl. All protein was concentrated to 150 μM using 30 kDa molecular weight cut-off Amicon Ultra-15 Centrifugal filter units. All purification steps were conducted at 4 °C.

***In vitro* ligand binding assays**. The interaction of steroid **12** and abiraterone (as a control) with recombinant human CYP17A1 and CYP3A4 was measured using differential spectrophotometric titration method. Difference spectra were recorded at 25 °C using dual-beam UV-Vis-NIR spectrophotometer Cary 5000 (Agilent Technologies, USA) equipped with temperature-controlled cuvette holders. All measurements were performed in 0.1 M potassium phosphate buffer (pH 7.4) with 0.15 M NaCl, 20% glycerol at 25 °C in the wavelength range of 350–500 nm. The protein concentration and optical path length were 1 μM and 1 cm, respectively. Abiraterone and tested compounds were dissolved in ethanol and in dimethylformamide, respectively. An equivalent amount of the appropriate solvent was added to the reference cuvette to eliminate solvent dependent difference spectrum perturbation. The total amount of solvent in the titration experiment did not exceed 2% of the sample volume.

For the titration curves fitting, the tight binding equation (Morison equation) was used:

$$\Delta A = \Delta A_{max}\left\{([P_T] + [L_T] + K_D) - \left[([P_T] + [L_T] + K_D)^2 - 4[P_T][L_T]\right]^{\frac{1}{2}}\right\}/2[P_T]$$

where ΔA is the observed absorbance change, ΔA_{max} is the maximum absorbance change, K_D is the apparent equilibrium dissociation constant, $[P_T]$ and $[L_T]$ are the total concentrations of CYP17A1/CYP3A4 and inhibitor, respectively. The fitting procedure was performed using the curve_fit function of the scipy.optimize module of python3 numpy library. All graphs were plotted using the matplotlib.pyplot library.

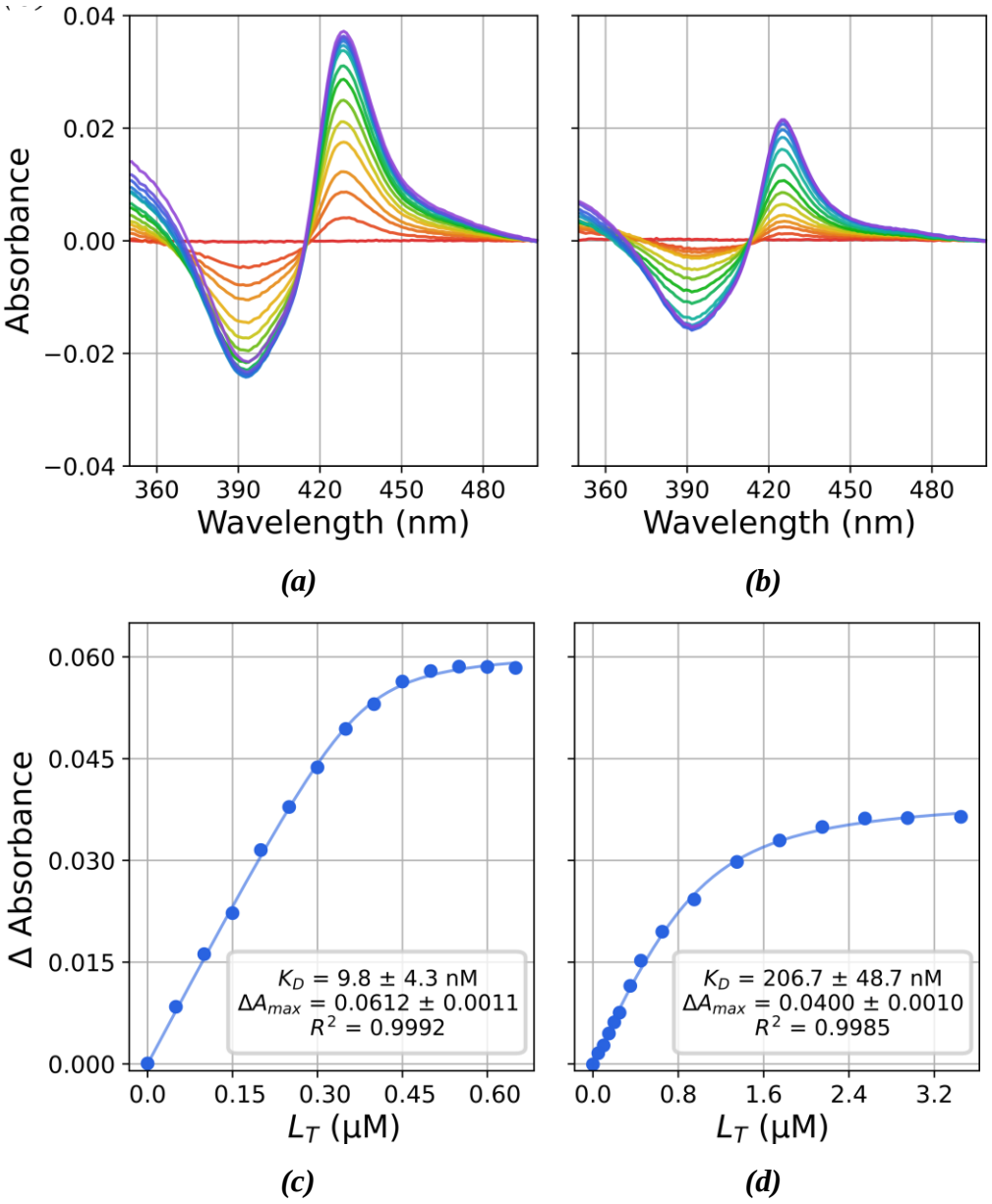

Figure S11 UV-visible differential spectrophotometric titration for equilibrium dissociation constant (K_D) determination. Absorbance change measured during the titration of CYP3A4 (1 μM) with compound **12** *(a)* or abiraterone (**1**) *(b)* and corresponding binding isotherms: for compound **12** *(c)* and abiraterone (**1**) *(d)*. ΔA_{max} is a maximum absorbance change and L_T is a total ligand concentration. The solid line on binding isotherms represents the nonlinear fit for K_D determination.

References

S1. O. Trott and A. J. Olson, *J. Comput. Chem*., 2010, **31**, 455; https://doi.org/10.1002/jcc.21334.

S2. E. F. Pettersen, T. D. Goddard, C. C. Huang, G. S. Couch, D. M. Greenblatt, E. C. Meng and T. E. Ferrin, *J. Comput. Chem*., 2004, **25**, 1605; https://doi.org/10.1002/jcc.20084.

S3. E. M. Gillam, T. Baba, B. R. Kim, S. Ohmori and F. P. Guengerich, *Arch. Biochem. Biophys*., 1993, **305**, 123; https://doi.org/10.1006/abbi.1993.1401.

S4. G. Habermehl and A. Haaf, *Liebigs Ann. Chem*., 1969, **723**, 181; https://doi.org/10.1002/jlac.19697230119.

S5. C. M. Kormos, M. G. Gichinga, S. P. Runyon, J. B. Thomas, S. W. Mascarella, A. M. Decker, H. A. Navarro and F. I. Carroll, *Bioorg. Med. Chem.*, 2016, **24**, 3842; https://doi.org/10.1016/j.bmc.2016.06.029.

S6. M. Simonetta and S. Winstein, *J. Am. Chem. Soc.*, 1954, **76**, 18; https://doi.org/10.1021/ja01630a004.

S7. N. DeVore and E. Scott, *Nature*, 2012, **482**, 116; https://doi.org/10.1038/nature10743.

S8. E. V. Nurieva, O. Yu. Kravtsova, A. V. Sydoriuk, E. V. Britikova, V. V. Britikov, N. A. Zefirov, E. R. Milaeva and O. N. Zefirova, *Mendeleev Commun.*, 2024, **34**, 502; https://doi.org/10.1016/j.mencom.2024.06.010.